

RESEARCH ARTICLE

Performance analysis of two-hop decode-amplify-forward relayed system in different fading conditions

Shivali G. Bansal and Jemal H. Abawajy*

Parallel and Distributed Computing Lab, School of Information Technology, Deakin University, Australia

ABSTRACT

Recent advances in the field of wireless communication have proven the importance of diversity in combating channel fading and improving the bit error rates (BERs). In this report, a dual-hop decode-amplify-forward (DAF) transmission system over Nakagami- m fading channel is studied. The DAF relay system is a hybrid of decode-and-forward and amplify-and-forward relay systems that shows the benefits of both decode-and-forward and amplify-and-forward relay systems and is also called hybrid relay system or hybrid DAF relay system. Signal-to-noise ratios and BERs for various system models with varying number of transmit and receive antennas have been discussed. The diversity is achieved in two ways: firstly, by the use of relay and secondly, by the use of multiple antennas at both the transmitter and the receiver. Dual-hop relaying gives better trunking efficiency and with single antenna at the relay site acquisition and antenna structures are much less expensive. The variations in the performance levels when the relay is moved to different locations within the line of sight of the transmitter and the receiver have also been analyzed. BERs with respect to variations in the fading parameter ' m ' have also been presented and discussed. Copyright © 2013 John Wiley & Sons, Ltd.

KEYWORDS

cooperative relaying; Nakagami- m fading channel; space-time block codes; maximum ratio combining; MPSK modulation

*Correspondence

Jemal H. Abawajy, Parallel and Distributed Computing Lab, School of Information Technology, Deakin University, Australia.

E-mail: jemal.abawajy@deakin.edu.au

1. INTRODUCTION

An insight into the current state of technology in wireless communication reveals that there are various ways by adopting which the performance of any wireless system can be significantly improved. Communication taking place over a wireless radio channel is limited by multipath, fading, interference, path loss, and shadowing [1]. By combining various modulation and coding techniques, by efficient channel estimation, and by considering the amount of diversity involved, [2], new communication systems can be modeled. Spatial diversity techniques have been widely exploited to battle multipath fading and other channel impairments. In recent advances, radio transceiver techniques such as multiple input multiple output (MIMO) system designs have shown tremendous improvement in the capacity of the current systems by dealing with the channel multipath fading [3–5].

Although the use of multiple antennas fulfilled the promise in mitigating the effects of fading, however, because of hardware complexity and bulky features [6],

use of MIMO systems seems impractical in *ad hoc* or distributed large scale wireless networks for certain applications. To meet the demands of increased reliability and spectral and power efficiency without increasing the size of mobile devices, we need fundamentally new paradigms to improve the system performance. Cooperative communications have been introduced in an effort to overcome these limitations and meet the growing demands. Cooperative communications has the ability to exploit the spatial diversity inherent in multiuser systems by allowing users with diverse channel qualities to cooperate and relay each other's messages to the destination [7]. Each transmitted message is passed through multiple independent relay paths, and thus, the probability that the message fails to reach the destination is significantly reduced. Spatial diversity can be achieved even if the user is equipped with only one antenna by relaying each other's message such as to form a distributed antenna array to achieve the diversity gain of a MIMO system capable of combating multipath fading in wireless channels. This is similar to realizing a virtual antenna array, thus achieving

cooperative diversity. This makes cooperative techniques attractive for deployment in cellular mobile devices as well as in *ad hoc* mobile networks [8]. The simplest example of a cooperative network is the relay-assisted communication, which has recently gained a lot of attention. Cooperative relaying has the potential of enhanced coverage, reliability, and throughput of wireless networks with strict spectrum and power constrictions. In contrast to conventional MIMO systems, the relay-assisted transmission is able to combat not only the small scale but also large scale effects such as shadowing and path loss. Thus, cooperative relaying has found applications in wireless cellular, *ad hoc*/wireless sensor networks, cognitive radio, Wi-Fi/Worldwide Interoperability for Microwave Access, and IEEE 802.11n [9]. These schemes efficiently deal with diversity via relayed transmission where a relay is used to transfer data from the transmitter to the receiver in addition to the direct transmission, thus exploiting diversity gained by multiple transmissions [10].

Cooperative relaying schemes can be categorized as amplify-forward (AF) [11], where the relay terminal simply amplifies the received signal and transmits it to the receiver, and decode-and-forward (DF) where the relay terminal decodes and then forwards the signal to the receiver [12]. DF can be further sub-categorized as fixed DF (FDF) and adaptive DF (ADF). Most of the systems modeled in the past based on these schemes assumed single transmit and receive antennas and single antenna-based relays. These systems were further elaborated by using multiple relays, but this added to the system cost and complexity of employing more number of antennas at the relay and increased number of tasks by every relay antenna, respectively. Relay-based systems were further enhanced by using multiple relays in MIMO systems. Although such systems gave higher performance, fear of failure of a single or multiple relays highly affected the performance of the system.

Convinced by the benefits of using AF and DF, a hybrid scheme combining AF and FDF with soft decision, namely, decode-amplify-forward (DAF) protocol, was presented in [13] and [14] over Rayleigh fading channels. This hybrid scheme cleverly combined the merits of both AF and FDF mode. In [14], it was mentioned that during the second-hop transmission, if the signal is corrupted as in the ADF protocol, in the hybrid relay system or hybrid DAF (HDAF) relay system scheme, the relay starts to perform in the AF mode. In this paper, emphasis on a two-hop DAF relay-based system is placed with a difference that at the transceiver (TR) node, that is, the relay, the received bits are decoded, estimated, demodulated, amplified, and then forwarded to the receiver. This system model maintains low complexity as the data bits are not encoded again at the TR node as is carried out in almost all the present relay-based systems. Also, the number of antennas at the TR node is kept low to one. However, the number of antennas at the transmitter and/or receiver can be varied, thus capable of forming a system model with any number of antennas at either end. Also, the system proves to be

dynamic that even if the TR node fails to perform because of any unavoidable circumstances, the transmission will still take place as a normal direct link communication between the transmitter and the receiver forming a conventional MIMO system. However, with multiple TR nodes, the probability of failure of all the TR nodes at once is low, and the proposed HDAF system is still expected to communicate cooperatively and efficiently with the remaining number of TR nodes. For simplicity, the number of TR nodes in this paper is kept to one, but the proposed system is expandable to TR nodes greater than one in number. Also, the system is able to have variable number of transmit and receive antennas without modifying the functionality of the TR node.

The remainder of this paper is organized as follows: Section 2 presents the related work. Section 3 presents the system model and the channel model describing the data transmission and signal processing with single/multiple transmit/receive antennas. In Section 4, the equivalent signal-to-noise ratio (SNR) description is provided for various system models. Section 5 presents the performance evaluations and the simulation parameters used for simulating various system models. Finally, Section 6 summarizes the findings of the research and concludes the paper.

2. RELATED WORK

Relay-based communication was first introduced in [15] and was further studied in [16]. The work was further extended by deriving upper and lower capacity bounds in [17], which provided an information-theoretic analysis for a one-way full-duplex relay channel under additive white Gaussian channels. Since then, cooperative relaying in communications has been a center of research in dealing with channel fading. Extensive works have been performed on analyzing the performance of conventional relay networks [18–20].

Recently, a new class of forwarding strategy, named as DAF, was proposed for relay channels. The proposed DAF strategy cleverly combined the merits of both DF and AF by exploiting the coding gain on the inter-user channel and maximizing the data reliability. Because this hybrid scheme combined the merits of both AF and DF relay schemes, it is also known as HDAF scheme. The HDAF scheme combining AF and FDF with soft decision, namely DAF protocol, has recently been reported in [13]. The relay performed soft decoding and forwarded the reliability information at the output of its decoder to the destination, hence combining both AF and DF mode. An HDAF protocol was also investigated in [21] for multiple parallel relays over independent and nonidentical distribution flat Rayleigh fading channels using maximum ratio combining (MRC). The closed form tight bounds were derived. It was also shown that the outage probability outperforms the DF protocol. Another hybrid scheme of ADF and AF for orthogonal frequency division multiplexing systems was proposed in [22]. Depending on the channel condition of

the source-to-relay link on each subcarrier, the better protocol between ADF and AF is selected. Simulation results verified the advantages of the proposed hybrid scheme. In [14], a cooperative communication scheme with HDAF protocol combining the AF mode and ADF mode with hard decision was focused on. It was shown that instead of remaining silent during the second-hop transmission, if the signal is corrupted as in the ADF protocol, the HDAF scheme can increase the performance by having the relay perform in the AF mode. When the relay has full knowledge about the instantaneous fading channel of the source-to-relay link, it can operate in channel state information-assisted AF relay mode. The performance gain of HDAF relay protocol over the ADF and AF in dual-hop multiple-relay networks was also investigated in [23]. The performance gain in terms of the symbol error probability in high SNR regime was analyzed. It was also shown that in contrast to the single-relay case in which the HDAF scheme has no benefit compared with ADF and AF as the relay is located close to the source, HDAF still achieves a small gain with multiple relays. In [24], the performance of HDAF protocol for linear block coded signals was analyzed. The findings showed the bounds for bit error rate (BER) over independent and identical distribution (i.i.d.) and that this protocol works better than the existing AF protocol. The BER and outage probability of HDAF over a conventional three node relay channel was analyzed in [25]. The paper analyzed the performance of SNR-based HDAF relaying cooperative diversity networks over independent nonidentical flat Rayleigh fading channels with MRC technique. Closed-form expressions for the outage and bit error probability of the HDAF relaying scheme were also derived.

In this paper, the hybrid DAF relay system for MIMO systems describing the relay as the TR node with single antenna capable of transmitting and receiving the information has been discussed. The system model under consideration works on the principle of FDF. The relaying principle described in [18] decodes and recodes the signal before forwarding it to the receiver, whereas in this paper, the TR node performs the task of decoding and estimating the received signal followed by demodulation and error check. During error check, the TR node amplifies the signal only when no error takes place. In case of any error detected, the TR node simply re-modulates the signal and forwards it to the receiver. However, the signal is never encoded again because of single relay antenna at the TR node.

A cooperative relay-based network with a large number of relay nodes transmitting over independent nonidentical Nakagami- m fading channels with AF has been discussed in [26]. The performances of FDF and ADF schemes over Nakagami- m fading channels have been analyzed and compared in [12] where the results were obtained considering that the m parameter of the fading channel is always an integer. In this paper, it is considered that the relay is capable of transmitting and receiving the information over Nakagami- m fading channel. Also, the error performances, where the fading parameters m_1 and m_2 of the channel

paths from the transmitter to the TR node ($T - TR$) and TR node to receiver ($TR - R$), respectively, can take any value from $0.65 \leq m \leq 10$, have been presented. Although m can take any rational value, the sum of these two fading parameters is always an integer. Also, the results in [12] were limited to binary phase shift keying (BPSK) modulation, whereas the system model described in this paper works for higher orders of PSK modulation as well. Also, to maintain the simplicity of the system, the TR node consists a single antenna relay. This makes the system dynamic as in case of any unlikely failure of the TR node, the communication can still take place by bypassing the TR node. The system model under investigation can be modified to a relay with multiple antennas or multiple relays with single antenna. Larger number of relays/antennas may help in performance improvement but may also result in significant drop in the performance if the link to the TR node fails, thus reducing the order of diversity.

3. SYSTEM AND CHANNEL MODEL

3.1. System model

Assuming that perfect channel state information is available at the receiver and known partially at the transmitter via a feedback channel, the system is modeled on the basis of the assumptions that the channel is quasi-static and flat-fading, and the transmit antennas to have equal transmission power. Transmit and receive diversity is exploited jointly by using space-time block codes (STBCs) at the transmitter side and MRC at the receiver side by using multiple antennas at both ends. The system model under consideration works on the principle of FDF. The relaying principle described in [18] decodes and recodes the signal before forwarding it to the receiver, whereas in this paper, the TR node performs the task of decoding and estimating the received signal followed by demodulation and error check. During error check, the TR node amplifies the signal only when no error takes place. In case of any error detected, the TR node simply re-modulates the signal and forwards it to the receiver. However, the signal is never encoded again because of single antenna at the TR node. The incoming data is carried over multiple data spatial streams depending on the number of antennas used. The initial 802.11n standard defined up to two spatial streams allowing the capacity to double, whereas the 802.11n standard finalized in 2009 allowed from three up to four data spatial streams over a 40 MHz wide channel. The proposed system allows up to three data spatial streams over three transmit and three receive antennas.

The proposed MIMO system transmission using the TR node is shown in Figure 1. The transmitter sends the information to the receiver following two paths: a direct path to the receiver and an indirect path via the TR node. For a system model with single transmit antenna, no coding is performed at the transmitter, and the whole system works

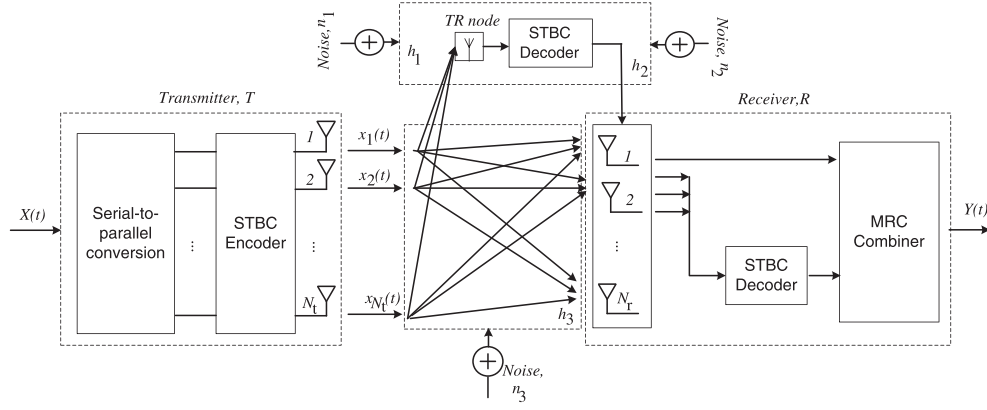


Figure 1. A MIMO communication model with additional TR node.

as an AF network where the TR node receives the signal, demodulates it, check for errors and re-modulates it, and then sends it to the receiver with errors, if any. The decoders shown in Figure 1 at the TR node and at the receiver are bypassed in a single antenna system model. For a system model with multiple transmit antennas, the signal to be transmitted is encoded using STBC and sent over the two channel paths. The received signal at the TR node is decoded and estimated, demodulated and checked for errors, re-modulated and then sent to the receiver. No error correction takes place at the TR node in any case.

At the receiver, all the information bearing signals, both from direct transmission and from the TR node are received by the receiving arrays. For a single input single output (SISO) system model, the signals received from the two sources are simply combined at the receiver. For a multiple input single output (MISO) system model, the received signals are sorted such that the signals received from direct transmission are sent to the decoder, whereas the signals received after transmission from the TR node are fed directly to the combiner. The decoder output is also sent to the combiner, and the signals received from two different sources are then combined. For a single input multiple output (SIMO) system models, the signals received from the TR node over all receive antennas are MRC combined separately, and those received from the direct transmission are MRC combined separately. For a MIMO system model, the signals received from the TR node are MRC combined, whereas those received directly from the transmitter are MRC combined and then decoded as well. The two signals from the TR node and from the transmitter are then summed up in all the cases and then demodulated to retrieve the actual information sent. Then, the number of errors occurred is calculated.

3.2. Channel model

Considering a receiver with M diversity branches, the received instantaneous signal A_k at the k^{th} branch can

be characterized by the Nakagami distribution with the probability distribution function given by

$$p_R(R_k) = \frac{2}{\Gamma m_k} \left(\frac{m_k}{\Omega_k} \right)^{m_k} r^{2m_k-1} e^{-\frac{m_k}{\Omega_k} r^2}, k=1, 2, \dots, M \quad (1)$$

where the amplitude $r \geq 0$, $\Gamma(\cdot)$ is the Gamma function, $\Omega_k = E(R_k^2) = \overline{R_k^2}$ is the average power on k^{th} branch, and m_k is the fading parameter. m is the inverse of the normalized variance of R^2 expressed as

$$m = \frac{(E(R^2))^2}{\text{Var}(R^2)} \quad (2)$$

where $\text{Var}(R^2)$ is the variance of R^2 . Typically, the value for m ranges between $1/2$ and ∞ . When $m \rightarrow \infty$, the channel converges a static channel. The Nakagami distribution is selected to fit empirical data and is known to provide a close match to some experimental data than the Rayleigh distributions. The Nakagami distribution is often used to model multipath fading as it can model fading conditions that are either more or less severe than Rayleigh fading. m is the Nakagami fading parameter that determines the severity of the fading. When $m = 1$, Nakagami distribution becomes the Rayleigh distribution; when $m = 1/2$, it becomes a one-sided Gaussian distribution; and when $m = \infty$, the distribution becomes an impulse (no fading). Even Rice distribution can be closely approximated using Nakagami parameter m via the relationship $m = (K + 1)^2 / (2K + 1)$. An optimum power loading algorithm for transmitter diversity systems over correlated and unbalanced Nakagami paths and its performance evaluation under perfect channel estimate conditions has been derived in [27]. In addition to this, various online estimators of the required Nakagami channel parameters for optimized power loading and the comparison of their mean square error via Monte Carlo simulations have also been presented. Because [19] presented the coefficients for finite values of m between 0.65 and 10 to minimize the approximation error, the target of the paper is to closely follow

the values of m in-between this range. The Nakagami distribution is related to the gamma distribution as can be seen from (1). Considering the channel model as shown in Figure 1, it can be illustrated that the severity of the fading depends on the distance between the transmitter and the receiver. Also, the $(T - TR)$ and $(TR - R)$ distance affects the level of fading as well as communication over larger distances are expected to suffer from deep fades because of channel impairments. Furthermore, the fading parameter m relates to the severity of fading, where lower values of m correspond to fading severe than Rayleigh fading and higher values of m corresponds to less severe fading than Rayleigh fading. Thus, a theoretical understanding and assumption can be made that for lower values of m , when the system is expected to suffer from higher fading, the two ends of the communication system are placed at a larger distance. In comparison, for higher values of m , the system suffers from less severe fading, and the two ends of the communication system can be assumed closer to each other.

For any wireless communication system with N_t transmit and N_r receive antennas communicating over i.i.d. Nakagami- m fading channel, the channel matrix H for the MIMO system can be defined as an $N_t \times N_r$ channel matrix whose entries are the fading coefficients $h_{i,j}$, $i = 1, \dots, N_t$, $j = 1, \dots, N_r$ and can be expressed as

$$H = \begin{bmatrix} h_{11} & \cdots & h_{1,N_r} \\ \vdots & \ddots & \vdots \\ h_{N_t,1} & \cdots & h_{N_t,N_r} \end{bmatrix} \quad (3)$$

where the amplitude of the channel fading coefficients follow Nakagami- m distribution with fading parameter $0.65 \leq m \leq 10$. At the receiving side, every receive antenna receives the direct components intended for it as well as the indirect components, which are meant for other receive antennas. Thus, by using the direct and the cross channel components, the channel transmission matrix of (3) is formed.

Considering Figure 1, the channel matrix H for the proposed system model can be defined as follows: from the source to the TR node, the communication takes place over channel h_1 . Thus, h_1 can be defined as a $N_t \times 1$ channel matrix whose entries are the fading coefficients $h_{i,1}$, $i = 1, \dots, N_t$. From the TR node to the destination, the communication takes place over h_2 , which can be defined as a $1 \times N_r$ channel matrix whose entries are the fading coefficients $h_{1,j}$, $j = 1, \dots, N_r$. Thus, the channel matrices h_1 and h_2 can be expressed as

$$h_1 = \begin{bmatrix} h_{11} \\ h_{21} \\ \vdots \\ h_{N_t,1} \end{bmatrix} \quad (4)$$

and

$$h_2 = [h_{11} h_{12} \dots h_{1,N_r}] \quad (5)$$

respectively, assuming that the two matrices are independent of each other. The direct transmission of information from transmitter to the receiver takes place via a direct path over the channel h_3 . Each of the h_1 , h_2 , and h_3 channel matrices consists of i.i.d. Nakagami- m channel coefficients. Also, h_3 is an $N_t \times N_r$ channel matrix, similar to (3).

3.3. Data transmission and processing

Considering x is the multiple phase shift keying (MPSK)-modulated signal to be transmitted; then during the first time slot, the transmitter sends the signal directly to the receiver over a direct channel path h_3 and to the TR node over another channel path h_1 . During the second time slot, the TR node sends the received signal to the receiver over channel path h_2 . The communication between the transmitter (T) and the TR node, TR node and the receiver (R), and direct communication between the transmitter and the receiver will be written as $(T - TR)$, $(TR - R)$, and $(T - R)$, respectively. The signals received between $(T - TR)$, $(TR - R)$, and $(T - R)$ experience independent fading and are normalized individually. With h_1 , h_2 , and h_3 being the channel coefficients for the paths between $(T - TR)$, $(TR - R)$, and $(T - R)$, respectively, and n_1 , n_2 , and n_3 being the additive white noises with zero mean and variance equal to N_0 for $(T - TR)$, $(TR - R)$, and $(T - R)$, respectively, the transmission takes place as follows:

3.3.1. Transmission over single transmit antenna.

The signals are transmitted with energy E_b using single transmit antenna over single radio frequency (RF) link, which has Nakagami- m distribution. Then, the signal received at the TR node from the transmitter is given by

$$y_{(T-TR)} = \sqrt{E_b} x h_1 + n_1 \quad (6)$$

Equalization is performed at the TR node by dividing the received signal $y_{(T-TR)}$ by the apriori known h_1

$$\hat{y}_{(T-TR)} = \frac{y_{(T-TR)}}{h_1} = \frac{x h_1 + n_1}{h_1} = x + \dot{n} \quad (7)$$

where $\dot{n} = \frac{n_1}{h_1}$ is the additive noise scaled by the channel coefficient h_1 . No decoding takes place at the TR node as the data sent was un-coded. Maximum likelihood

demodulation of the signal $\hat{y}_{(T-TR)}$ is performed as follows:

$$(\hat{y}_{(T-TR)})_{\text{est}} = (\hat{y}_{(T-TR)} - MPSK_{\text{mapset}})' \cdot (\hat{y}_{(T-TR)} - MPSK_{\text{mapset}}) \quad (8)$$

where $MPSK_{\text{mapset}} \in \begin{cases} \{0, 1\} & \text{when } M = 2 \\ \{0, 1, 2, 3\} & \text{when } M = 4, \\ \text{and so on for higher modulations.} \end{cases}$

The decision is made in favor of the symbol with minimum distance to retrieve the signal with minimum number of errors as

$$\hat{x} = \min (\hat{y}_{(T-TR)})_{\text{est}} \quad (9)$$

3.3.2. Transmission over multiple transmit antennas.

The signals are transmitted over multiple transmit antennas, and the received signal at the TR node can be written as

$$y_{(T-TR)} = \sqrt{E_b} G_{N_t}^* h_1 + n_1 \quad (10)$$

where $G_{N_t}^*$ is the encoder matrix and is based on the orthogonal design rule such that $G_{N_t} G_{N_t}^H = (|x_1|^2 + |x_2|^2 + \dots + |x_k|^2) \mathbf{I}$ to achieve full transmit diversity of N_t . $G_{N_t}^H$ is the hermitian transpose of G_{N_t} , and \mathbf{I} is the $N_t \times N_t$ identity matrix. When $N_t = 2$, $G_{N_t}^*$ is given by [28]

$$G_2^* = \begin{pmatrix} x_1 & x_2 \\ -x_2^* & x_1^* \end{pmatrix} \quad (11)$$

When $N_t = 3$, $G_{N_t}^*$ is given by

$$G_3^* = \begin{bmatrix} x_1 & -x_2 & -x_3 & -x_4 & x_1^* & -x_2^* & -x_3^* & -x_4^* \\ x_2 & x_1 & x_4 & -x_3 & x_2^* & x_1^* & x_4^* & -x_3^* \\ x_3 & -x_4 & x_1 & x_2 & x_3^* & -x_4^* & x_1^* & x_2^* \end{bmatrix} \quad (12)$$

The signal received at the TR node is decoded, estimated, and demodulated as follows:

$$\hat{y}_{(T-TR)} = x + (\tilde{H}_1^H \tilde{H}_1)^{-1} \tilde{H}_1^H n_1 \quad (13)$$

$$\hat{y}_{(T-TR)} = \begin{bmatrix} x_1 \\ x_2 \end{bmatrix} + \dot{n} \quad (14)$$

where $\dot{n} = (\tilde{H}_1^H \tilde{H}_1)^{-1} \tilde{H}_1^H n_1$ and $(\tilde{H}_1^H \tilde{H}_1)^{-1} \tilde{H}_1^H$ is the pseudo inverse of H_1 and $(\tilde{H}_1^H \tilde{H}_1)^{-1} = \left(\frac{1}{\sum_{i=1}^{N_t} \|h_{1i}\|^2} \right) \mathbf{I}$.

As the signal is received at the receiver, the demodulator examines the received symbol corrupted by the channel or the receiver. During the maximum likelihood detection,

the demodulator selects that point on the constellation diagram as its estimate of actually transmitted symbol, which

is closest to the received symbol in terms of the minimum Euclidean distance on the constellation diagram. At this point, if the corruption caused the received symbol to shift closer to any other constellation point than the one transmitted, it will incorrectly demodulate the symbol.

Assuming that the channel coefficients are constant over the p received symbols and starting with square transmission matrix, let ϵ_t denote the permutations of the first column to the t -th column and $\epsilon_t(i)$ denote the row position of x_i in the t -th column. Then, the Maximum likelihood (ML) detection rule is to form the decision variables

$$\tilde{x}_i = \sum_{t=1}^{N_t} \sum_{j=1}^{N_r} y_j^t h_{j, \epsilon_t(i)}^* \delta_t(i) \quad (15)$$

where $\delta_t(i)$ is the sign of x_i in the t -th column and $i = 1, 2, \dots, N_t$ and then deciding on the constellation symbol x_i that satisfies

$$\hat{x}_i = \arg \min_{c \in \mathcal{A}} Q \quad (16)$$

where $Q = (|\tilde{x}_i - c|^2 + (-1 + \sum_{j=1}^{N_r} \sum_{i=1}^{N_t} |h_{i,j}|^2) |c|^2)$ with \mathcal{A} the constellation alphabet. For MPSK signal constellation, $(-1 + \sum_{j=1}^{N_r} \sum_{i=1}^{N_t} |h_{i,j}|^2) |c|^2$ are constant for all signal points, given $h_{i,j}$. Therefore, the decision rule in (16) can be further simplified to

$$\hat{x}_i = \arg \min_{c \in \mathcal{A}} (|\tilde{x}_i - c|^2) \quad (17)$$

At this stage, no error correction is performed at the TR node.

3.3.3. Reception with single receive antenna.

The erroneous estimated signal \hat{x} (with the possibility of some errors) at the TR node is transmitted to the receiver over the channel path h_2 . The signal received at the receiver from the TR node is then given by

$$y_{(TR-R)} = \sqrt{E_b} \hat{x} h_2 + n_2 \quad (18)$$

The received signal y_{TR-R} is equalized and is given by

$$\hat{y}_{(TR-R)} = \frac{y_{(TR-R)}}{h_2} = \frac{\hat{x} h_2 + n_2}{h_2} = \hat{x} + \ddot{n} \quad (19)$$

where $\ddot{n} = \frac{n_2}{h_2}$ is the additive noise scaled by the channel coefficient h_2 . The signal received at the receiver directly from the transmitter is given by

$$y_{(T-R)} = \sqrt{E_b} x h_3 + n_3 \quad (20)$$

which is again individually normalized as

$$\hat{y}_{(T-R)} = \frac{y_{T-R}}{h_3} = \frac{xh_3 + n_3}{h_3} = x + \ddot{n} \quad (21)$$

where $\ddot{n} = \frac{n_3}{h_3}$ is the additive noise scaled by the channel coefficient h_3 .

3.3.4. Reception with multiple receive antennas.

The received signal is combined at the receiver using MRC to maximize the SNR and is given by the following expression:

$$\tilde{y}(t) = \sum_{j=1}^{n_R} h_j^* y_j(t) = x(t) \sum_{j=1}^{n_R} |h_j|^2 + n'(t) \quad (22)$$

In terms of the weight vector w , where $w = h^H$, the output x at the receiver is given by

$$x = \sqrt{E_s} h^H h x + h^H n \quad (23)$$

where $h^H h = \sum_{j=1}^{n_R} |h_j|^2$ is the sum of the channel powers across all the receive antennas. Thus, the signals coming from the TR node and directly from the transmitter after MRC and matched filtering are given by

$$\tilde{y}_{(TR-R)}(t) = \left(\sum_{j=1}^{n_R} |h_{2j}|^2 \right) \hat{x}(t) + \ddot{n}(t) \quad (24)$$

and

$$\tilde{y}_{(T-R)}(t) = \left(\sum_{j=1}^{n_R} |h_{3j}|^2 \right) x(t) + \ddot{n}(t) \quad (25)$$

respectively, where $\ddot{n}(t) = [n_{21}(t) \ n_{22}(t)]^T$ and $\ddot{n}(t) = [n_{31}(t) \ n_{32}(t)]^T$ are the complex noise vectors. It is worthwhile to note here that the copies of the signals received at the receiver from the TR node and from T are MR combined separately.

At the receiver, the received signals $\hat{y}_{(TR-R)}$ and $\hat{y}_{(T-R)}$ are summed as

$$Y = \text{sum}(\hat{y}_{(TR-R)}, \hat{y}_{(T-R)}) \quad (26)$$

Maximum likelihood demodulation of the signal Y is performed as follows:

$$(Y)_{\text{est}} = |Y - MPSK_{\text{mapset}}|^2 \quad (27)$$

The decision is again made in favor of the symbol with minimum distance to retrieve the signal with minimum number of errors as

$$X = \arg \min_{MPSK_{\text{mapset}} \in \mathcal{A}} (Y_{\text{est}}) \quad (28)$$

4. EQUIVALENT SIGNAL-TO-NOISE RATIO DESCRIPTION

The SNR of the (T – R) link is given by

$$\gamma_{(T-R)} = \frac{E_b}{N_0} \|H\|_F^2 \quad (29)$$

where $\|H\|_F^2 = \sum_{i=1}^{N_t} \sum_{j=1}^{N_r} \|h_{i,j}\|^2$, F is the Frobenious norm of H , and $\frac{E_b}{N_0}$ is the average SNR of the (T – R) channel represented by γ_3 . The TR node forwards the received signal to R with errors. R then combines the two signals by applying MRC followed by ML demodulation. The (T – TR) link and the (TR – R) link undergo independent Nakagami- m fading; thus, the received SNR $\gamma_{(T-TR)}$ and $\gamma_{(TR-R)}$ for each link, respectively, is gamma distributed with parameters α and β . Under this system, we consider the following unified model for the received SNR of the (T – TR – R) link

$$\gamma_{(TR)} = \frac{\gamma_{(T-TR)} \cdot \gamma_{(TR-R)}}{a\gamma_{(T-TR)} + \gamma_{(TR-R)} + b} \quad (30)$$

The parameters a and b are real and nonnegative and chosen such as to reflect the configuration of the TR node [29]. For a channel-assisted transmission, this configuration can be represented as $(a, b) \in (0, 1)$. Thus, (30) can be re-written as

$$\gamma_{(TR)} = \frac{\gamma_{(T-TR)} \cdot \gamma_{(TR-R)}}{\gamma_{(T-TR)} + \gamma_{(TR-R)}} \quad (31)$$

Thus, the equivalent end-to-end SNR at R is given by

$$\gamma_{\text{eq}} = \gamma_{(T-R)} + \gamma_{(TR)} \quad (32)$$

$$\gamma_{\text{eq}} = \gamma_{(T-R)} + \frac{\gamma_{(T-TR)} \cdot \gamma_{(TR-R)}}{\gamma_{(T-TR)} + \gamma_{(TR-R)}} \quad (33)$$

4.1. Equivalent signal-to-noise ratio for single input single output systems

For $N_t = 1$ and $N_r = 1$, (31) can be written as

$$\gamma_{(T-TR)} = \gamma_1 \|h_1\|^2 \quad (34)$$

$$\gamma_{(TR-R)} = \gamma_2 \|h_2\|^2 \quad (35)$$

$$\gamma_{(T-R)} = \gamma_3 \|h_3\|^2 \quad (36)$$

for (T – TR), (TR – R), and (T – R) channel paths where $\gamma_{(T-TR)}$, $\gamma_{(TR-R)}$, and $\gamma_{(T-R)}$ are the equivalent instantaneous SNRs, and γ_1 , γ_2 , and γ_3 are the average SNRs

of the (T – TR), (TR – R), and (T – R) channels, respectively. Thus, the equivalent SNR for a SISO system can be expressed as

$$\gamma_{\text{eq}} = \gamma_3 \|h_3\|^2 + \frac{\gamma_1 \|h_1\|^2 \cdot \gamma_2 \|h_2\|^2}{\gamma_1 \|h_1\|^2 + \gamma_2 \|h_2\|^2} \quad (37)$$

4.2. Equivalent signal-to-noise ratio for multiple input single output systems

For $N_t = i$ and $N_r = 1$, for direct transmission between the transmitter and the receiver with STBC, the received signal energy ($E_{r,1}$) and the received noise energy ($N_{0,1}$) for the first symbol estimate can be evaluated as

$$\begin{aligned} E_{r,1} &= E \left\{ \left(\sum_{i=1}^{N_t} \|h_{i,1}\|^2 \right)^2 x_1 x_1^* \right\} \\ &= \left(\sum_{i=1}^{N_t} \|h_{i,1}\|^2 \right)^2 E_{x1} \end{aligned} \quad (38)$$

and

$$N_{0,1} = N_0 \left(\sum_{i=1}^{N_t} \|h_{i,1}\|^2 \right) \quad (39)$$

Similarly, the received signal energy ($E_{r,2}$) and the received noise energy ($N_{0,2}$) for the second symbol estimate can be evaluated as

$$\begin{aligned} E_{r,2} &= E \left\{ \left(\sum_{i=1}^{N_t} \|h_{i,1}\|^2 \right)^2 x_2 x_2^* \right\} \\ &= \left(\sum_{i=1}^{N_t} \|h_{i,1}\|^2 \right)^2 E_{x2} \end{aligned} \quad (40)$$

and

$$N_{0,2} = N_0 \left(\sum_{i=1}^{N_t} \|h_{i,1}\|^2 \right) \quad (41)$$

Assuming $E_b = E_{x1} = E_{x2}$, the received symbol SNR can be written as

$$\gamma = \frac{E_{r,1}}{N_{0,1}} = \frac{E_{r,2}}{N_{0,2}} = \frac{E_b}{N_0} \left(\sum_{i=1}^{N_t} \|h_{i,1}\|^2 \right) \quad (42)$$

Thus, following (33), the equivalent end-to-end SNR at R for a wireless system with $N_t = 2$ and $N_r = 1$ is given by

$$\begin{aligned} \gamma_{\text{eq}} &= \gamma_3 \left(|h_{31}|^2 + |h_{32}|^2 \right) \\ &+ \frac{\gamma_1 \left(|h_{11}|^2 + |h_{12}|^2 \right) \cdot \gamma_2 \|h_2\|^2}{\gamma_1 \left(|h_{11}|^2 + |h_{12}|^2 \right) + \gamma_2 \|h_2\|^2} \end{aligned} \quad (43)$$

and when $N_t = 3$ and $N_r = 1$, the equivalent end-to-end SNR at R can be written as

$$\begin{aligned} \gamma_{\text{eq}} &= \gamma_3 \left(|h_{31}|^2 + |h_{32}|^2 + |h_{33}|^2 \right) \\ &+ \frac{\gamma_1 \left(|h_{11}|^2 + |h_{12}|^2 + |h_{13}|^2 \right) \cdot \gamma_2 \|h_2\|^2}{\gamma_1 \left(|h_{11}|^2 + |h_{12}|^2 + |h_{13}|^2 \right) + \gamma_2 \|h_2\|^2} \end{aligned} \quad (44)$$

and so on for higher orders.

4.3. Equivalent signal-to-noise ratio for single input multiple output systems

In the presence of channel h_j , the instantaneous SNR at j^{th} receive antenna is given by

$$\gamma_j = \frac{|h_j|^2 E_b}{N_0} \quad (45)$$

With N_r receive antennas, the effective SNR is given by

$$\gamma_{b_j} = \sum_{j=1}^{N_r} |h_j|^2 \frac{E_b}{N_0} \quad (46)$$

$$\gamma_{b_j} = N_r \gamma_j \quad (47)$$

For example, when $N_t = 1$ and $N_r = 2$, γ_{eq} can be expressed as

$$\begin{aligned} \gamma_{\text{eq}} &= \gamma_3 \left(\|h_{31}\|^2 + \|h_{32}\|^2 \right) \\ &+ \frac{\gamma_1 \|h_{11}\|^2 \cdot \gamma_2 \left(\|h_{21}\|^2 + \|h_{22}\|^2 \right)}{\gamma_1 \|h_{11}\|^2 + \gamma_2 \left(\|h_{21}\|^2 + \|h_{22}\|^2 \right)} \end{aligned} \quad (48)$$

and when $N_t = 1$ and $N_r = 3$, the equivalent end-to-end SNR at R can be written as

$$\begin{aligned} \gamma_{\text{eq}} &= \gamma_3 \left(\|h_{31}\|^2 + \|h_{32}\|^2 + \|h_{33}\|^2 \right) \\ &+ \frac{\gamma_1 \|h_{11}\|^2 \cdot \gamma_2 \left(\|h_{21}\|^2 + \|h_{22}\|^2 + \|h_{23}\|^2 \right)}{\gamma_1 \|h_{11}\|^2 + \gamma_2 \left(\|h_{21}\|^2 + \|h_{22}\|^2 + \|h_{23}\|^2 \right)} \end{aligned} \quad (49)$$

and so on for higher number of receive antennas in the receiving array.

4.4. Equivalent signal-to-noise ratio for multiple input multiple output systems

The equivalent SNR for a MIMO system using TR node can be described depending on the number of transmit and receive antennas used in the array. Thus, with N_t transmit and N_r receive antennas, the SNR of the (T – R) link is given by

$$\gamma_{(T-R)} = \gamma_3 \sum_{i=1}^{N_t} \sum_{j=1}^{N_r} \|h_{3i}^j\|^2 \quad (50)$$

The SNR of the (T – TR) link is given by

$$\gamma_{(T-TR)} = \gamma_1 \sum_{i=1}^{N_t} \|h_{1i}\|^2 \quad (51)$$

The SNR of the (TR – R) link is given by

$$\gamma_{(TR-R)} = \gamma_2 \sum_{j=1}^{N_r} \|h_{2j}\|^2 \quad (52)$$

and the equivalent SNR can be written as

$$\gamma_{eq} = \gamma_3 \sum_{i=1}^{N_t} \sum_{j=1}^{N_r} \|h_{3i}^j\|^2 + \frac{\gamma_1 \sum_{i=1}^{N_t} \|h_{1i}\|^2 \cdot \gamma_2 \sum_{j=1}^{N_r} \|h_{2j}\|^2}{\gamma_1 \sum_{i=1}^{N_t} \|h_{1i}\|^2 + \gamma_2 \sum_{j=1}^{N_r} \|h_{2j}\|^2} \quad (53)$$

5. PERFORMANCE EVALUATION

In this section, we present the simulation results for the models discussed in the previous sections.

Table I. Set of simulation parameters used.

Parameters	Types/values
Channel type	Quasi-static
Channel statistics	Nakagami- m
Fading parameter range	$0.65 \leq m \leq 10$
Number of frames	10^3
Frame length	100
Modulation type	MPSK (for $M = 2$ and 4)
Mathematical software used	MATLAB

5.1. Experimental setup

The parametric values used for simulation have been summarized in Table I. Monte Carlo method has been used for simulating. The results have been limited to $M = 2$ and 4, and the extension to higher modulation orders of $M > 4$ is straightforward. For the communication system equipped with N_t transmit and N_r receive antennas, the number of spatial data streams is typically calculated as $N_s = \min(N_t, N_r)$. On the basis of this, the proposed model is capable of defining up to three spatial data streams.

5.2. Results for two-hop decode-amplify-forward relay system for single input single output system models

Starting with a SISO system, a single data stream is transmitted from the transmitter equipped with single antenna. Figure 2 shows the BER of the proposed SISO system and compares it with the baseline approach. Figure 2(i, ii) shows the BER when the simulations were carried out for a BPSK and quadrature phase shift keying (QPSK) modulated sequences, respectively. It was shown in [30] that the Symbol error rate (SER) degrades with the increase in the number of relays at low values of SNR. Thus, we have assumed that the TR node consists of a single relay capable of receiving and forwarding the information. We see that with the added diversity at the receiver side from the TR node, the performance of the system improves by approximately 1 dB as compared to the conventional SISO transmission model for both BPSK and QPSK modulation. The fading parameter was kept at one for all the available channel paths of both the SISO models to obtain the results in Figure 2.

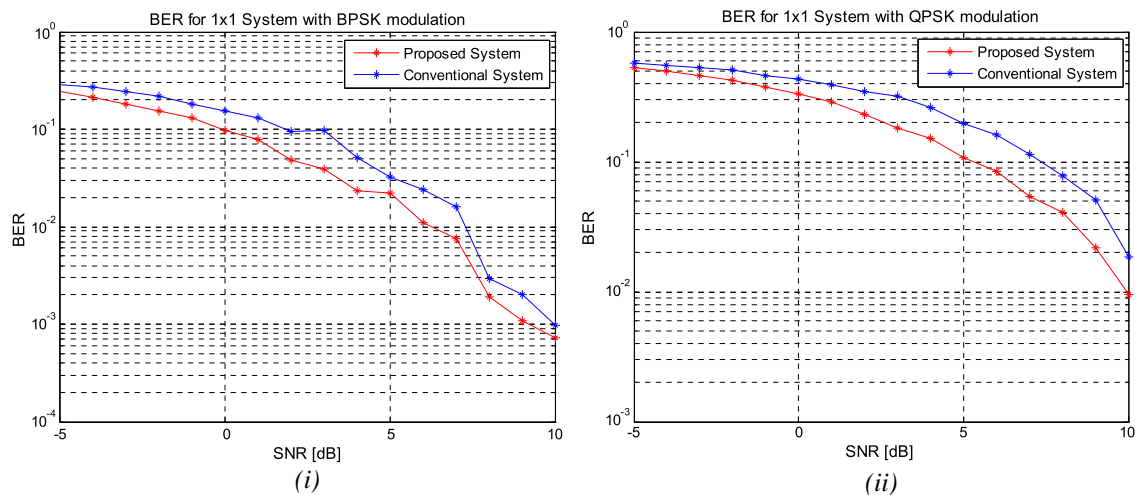


Figure 2. BER of the proposed SISO System with $m = 1$ for (i) BPSK and (ii) QPSK modulated Nakagami- m faded channel model and its comparison with the baseline model.

Figure 3 shows the performance of the proposed SISO system with different values of fading parameter. According to the path loss models, the performance of the system is improved as the distance between the transmitter and the receiver is decreased. In [31], the impact of variations in Nakagami- m fading parameter with distance has been investigated over frequency selective Nakagami fading channel, and it was observed that the operations at shorter distances gave better error rate performance. Hence, we assume that a higher fading parametric value means a shorter distance between the transmitter and the receiver.

On the basis of this assumption, we analyze the performance of the system with varying fading parameter. We refer the fading parameters for different channel links as follows: (i) fading parameter for the direct (T – R) link

is m_0 ; (ii) fading parameter for (T – TR) link is m_1 ; and (iii) fading parameter for (TR – R) link is m_2 .

Also, m_1 and m_2 can take any value from $0.65 \leq m \leq 10$, but $m_1 + m_2$ is always an integer and also $(m_1 + m_2) > 1$, as m_1 and m_2 are always greater than 0.65. Figure 3(i) shows the performance of the system when $m_0 = 1$ and $(m_1 + m_2) = 2$. With different values of fading parameter, it can be seen that the proposed SISO system gives the best performance when the fading conditions of both (T – TR) and (TR – R) link is Rayleigh, that is, $m_1 = m_2 = 1$. For the cases when the amount of fading on the two channel links is not same, the system gives better performance when $m_1 > m_2$. This can be explained on the basis of the assumption that higher fading parameter means less distance between the two links, thus, with $m_1 = 1.3$ and $m_2 = 0.7$, means that the

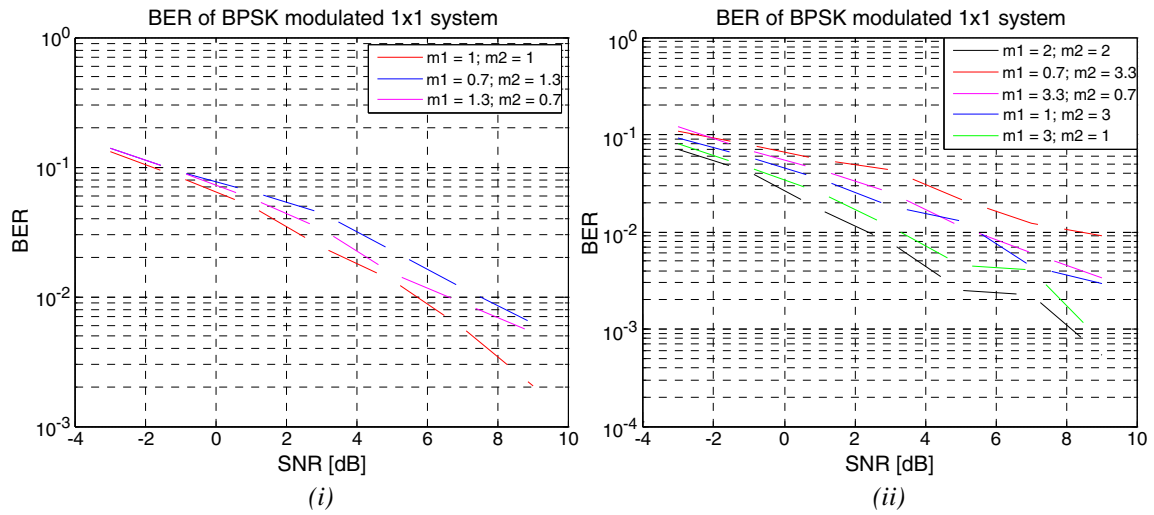


Figure 3. (i–ii) Performance analysis of the proposed SISO System with different fading parameters.

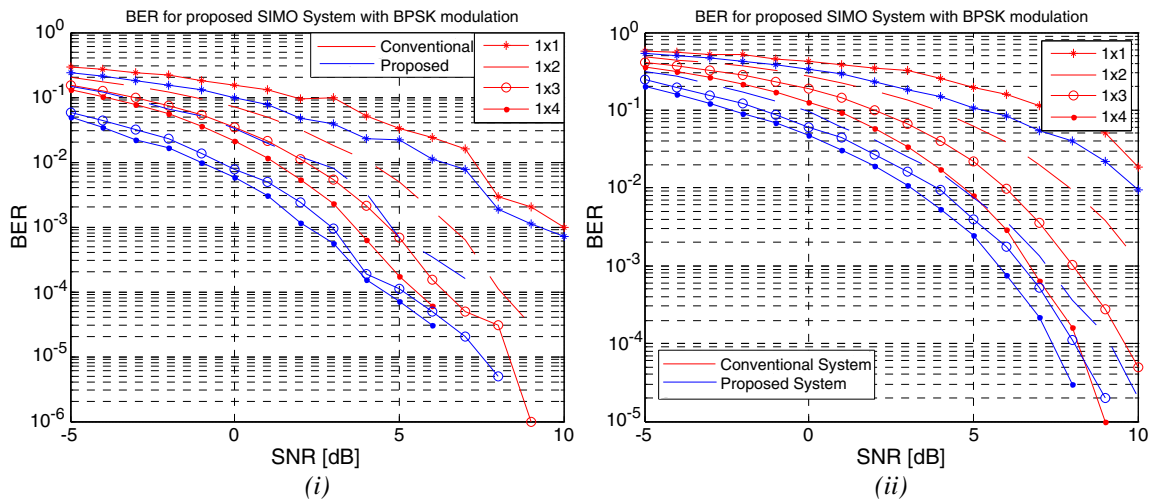


Figure 4. BER of the proposed SIMO System with $m = 1$ for (i) BPSK and (ii) QPSK modulated Nakagami- m faded channel model and its comparison with the baseline model.

distance between (T–TR) link is shorter than the (TR–R) link. The signals received directly from the transmitter and that from the TR node are combined at the receiver; thus, when the TR node is placed at a farther distance from the transmitter, the fading effects of the (T–TR) are stronger than the case when the TR node is placed closer to the transmitter. At the receiver, even if the TR node is placed farther from the receiver, the fading effects are reduced as the incoming signals from both the paths are combined. As can be seen from Figure 3(i), $m_1 = 0.7$ means higher fading effects and lower performance, and even though $m_2 = 0.7$, the system still shows a better performance as the fading effects are compensated by the combining of the signal at the receiver. Figure 3(ii) shows the BER when the fading conditions of both (T–TR) and (TR–R) links are less severe than Rayleigh, that is, $m_1 = m_2 = 2$, and comparing it with the BER when $m_1 \neq m_2$ but in all the case

$m_1 + m_2 = 4$. The simulation results show that the system gives the best performance when $m_1 = m_2$. When comparing the BER when $m_1 \neq m_2$, it can be seen that a better performance is achieved when the fading conditions on the (T–TR) link are less severe. For example, when $m_1 = 0.7$, the performance of the system degrades as compared with when $m_1 = 1$. It can also be noted that the performance of the system somehow depends on the fading conditions of the (TR–R) link. With $m_2 = 0.7$, the performance degrades as compared with when $m_2 = 1, 2, 3$.

5.3. Results for two-hop decode-amplify-forward relay system for single input multiple output system models

A single data stream is transmitted from single antenna and received over the receiver equipped with two receive

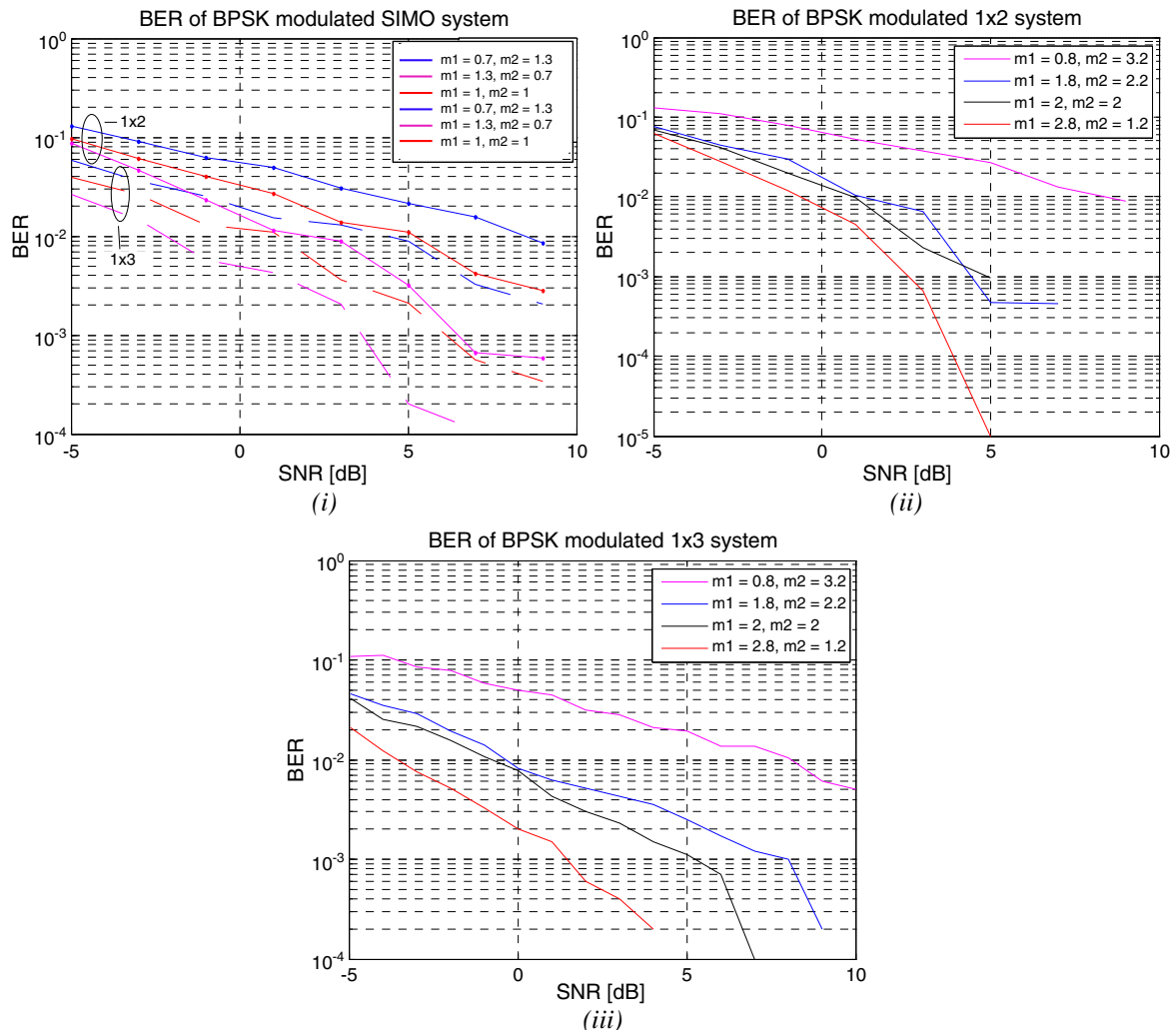


Figure 5. Effect of fading parameter on the performance of the proposed SIMO system. (i) BER of BPSK modulated SIMO system, (ii) BER of BPSK modulated 1 × 2 system, and (iii) BER of BPSK modulated 1 × 3 system.

antennas. Figure 4 shows the BER of the proposed SIMO systems and compares its performance with the baseline approach for BPSK and QPSK modulated sequences. With $m_0 = m_1 = m_2 = 1$, the simulations were carried out for 1, 2, 3, and 4 receive antennas. As can be seen from the figure at lower SNRs, the proposed system shows a performance improvement of approximately 2 dB but at higher SNR values; the performance slightly degrades but still shows an improvement of approximately 1 dB when compared with the baseline SIMO system models, for both BPSK and QPSK modulation.

By varying m_1 and m_2 such that $m_1 + m_2 = 2$ in Figure 5(i), it can be seen that the performance of the

system is improved when $m_1 > m_2$. As mentioned earlier, one of the many reasons for better performance is shorter distance between the transmitter and the receiver; thus, when the TR node is placed closer to the transmitter (higher m_1), the fading conditions on the (T – TR) link improve. At the receiver, although the distance between (TR – R) gets larger (lower m_2), MRC combining compensates for the poor fading conditions of the (TR – R) link. Figure 5(ii, iii) shows the BER for 2 and 3 receive antennas and shows similar pattern of results with m_1 and m_2 taking different values such that $m_1 + m_2 = 4$. It can be seen that the performance of the system is better when $m_1 > m_2$.

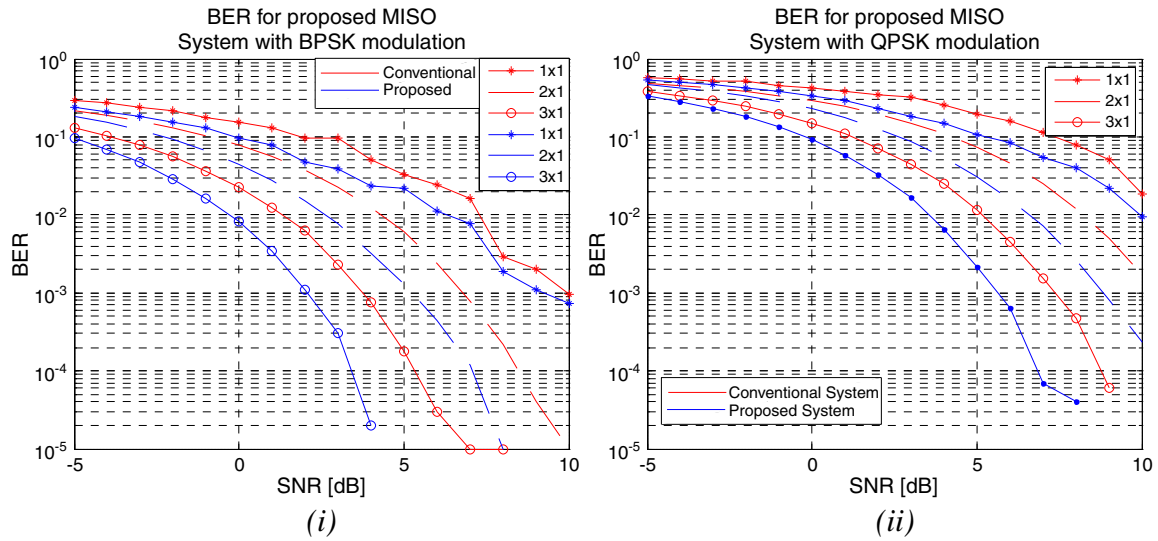


Figure 6. BER of the proposed MISO system with $m = 1$ for (i) BPSK and (ii) QPSK modulated Nakagami- m faded channel model and its comparison with the baseline model.

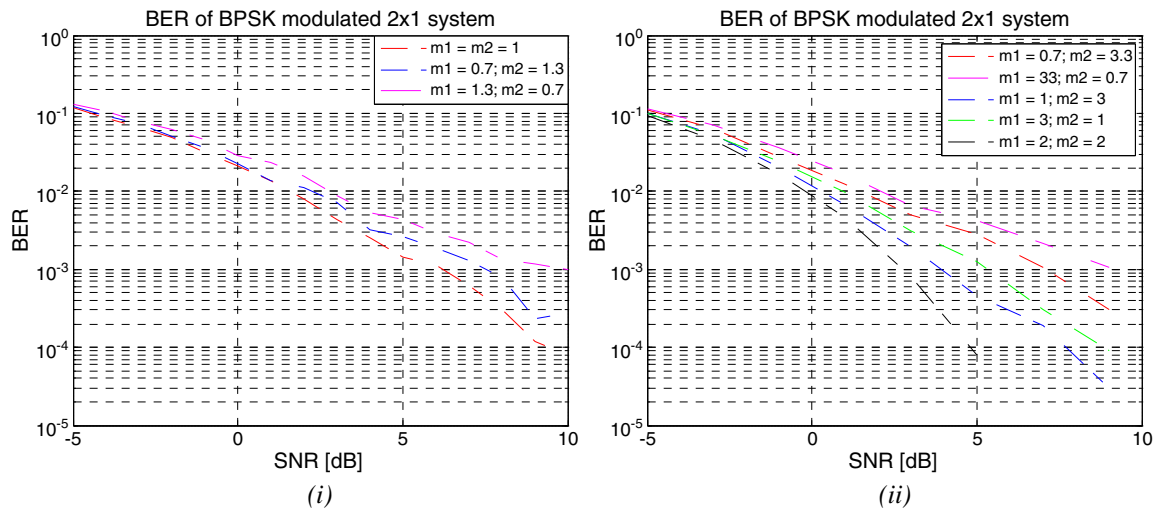


Figure 7. (i–ii) Effect of fading parameter on the performance of the proposed 2×1 system.

5.4. Results for two-hop decode-amplify-forward relay system for multiple input single output system models

Figure 6 shows the BER for the proposed MISO system. The simulations were carried out for 1, 2, and 3 transmit antennas. The BERs were calculated for both BPSK and QPSK modulated data sequences as shown in Figure 6(i, ii), respectively. It can be seen that with added diversity, the performance of the system is increased by approximately 1.5 dB as compared with the conventional MISO wireless system [8] for both BPSK and QPSK modulated systems.

Figure 7 compares the BER of 2×1 system for different fading conditions. Figure 7(i) plots the BER for varying

m_1 and m_2 with $m_1 + m_2 = 2$. It shows that in this case, the BER improves when $m_1 < m_2$, which is in contrast with the SIMO model where the performance improves when $m_1 > m_2$. It can be explained as follows: with multiple transmit antennas transmitting towards the TR node, the signals are MRC combined, so even if the TR node is placed at a larger distance from the transmitter than from the receiver, the higher fading effects are tolerated because of the MRC taking place at the TR node. At the receiver, if the distance between (TR – R) is larger than (T – TR), the fading effects of the (TR – R) are not efficiently compensated by the receiver. Thus, the proposed system shows degraded performance when $m_1 > m_2$, and the performance improves when $m_1 < m_2$. However, the

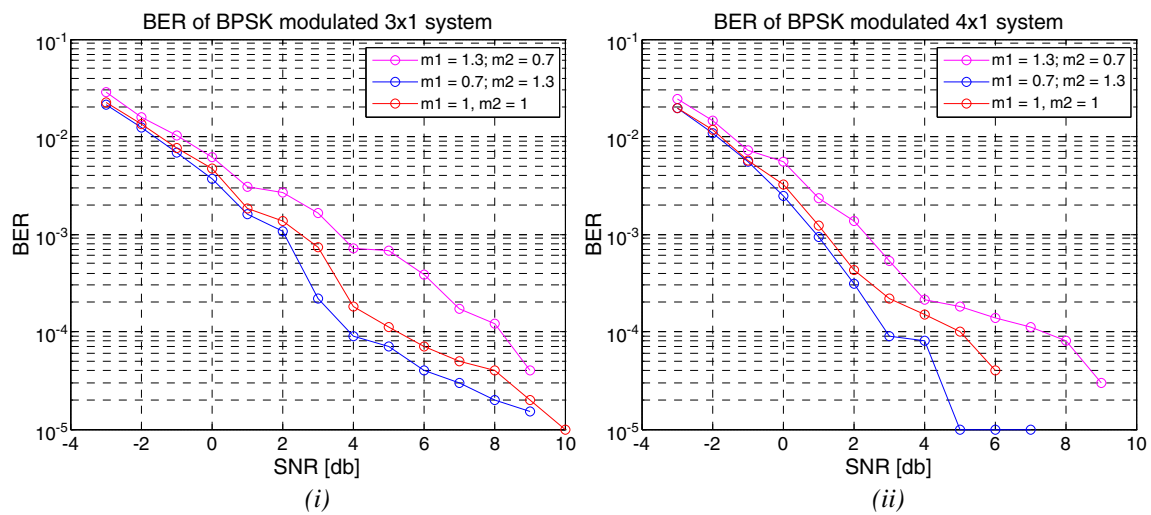


Figure 8. Effect of fading parameter on the performance of the proposed (i) 3×1 and (ii) 4×1 systems.

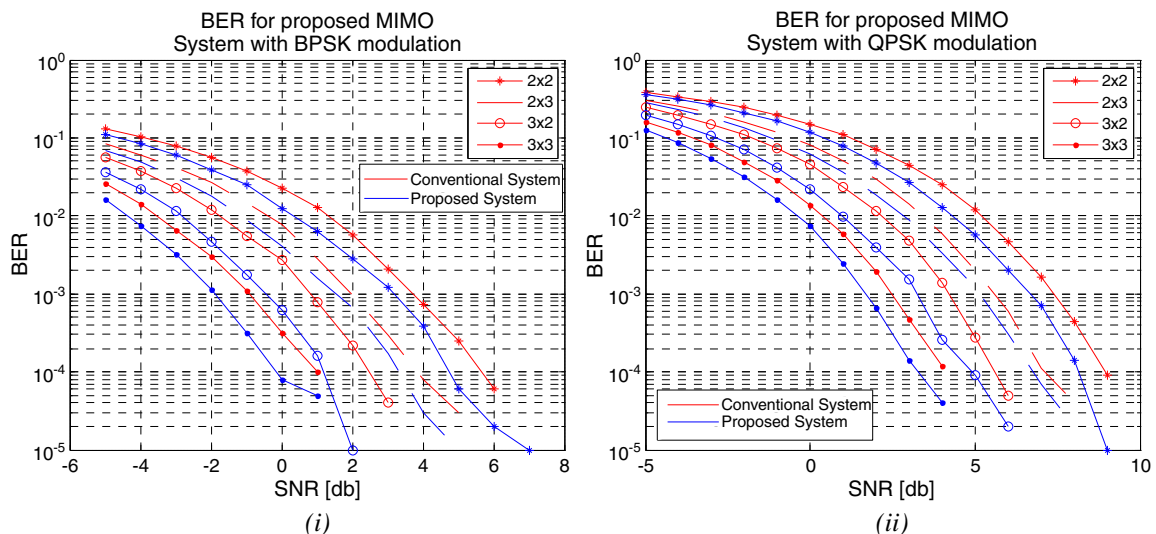


Figure 9. BER of the proposed MIMO System with $m = 1$ for (i) BPSK and (ii) QPSK modulated Nakagami- m faded channel model and its comparison with the baseline model.

best performance is achieved when $m_1 = m_2$. Figure 7(ii) shows the BER for BPSK modulated system for varying m_1 and m_2 with $m_1 + m_2 = 4$.

From the simulation plots, we analyzed that the best performance is achieved when both (T – TR) and (TR – R) links experience similar fading conditions. For the case when larger than $m_1 \neq m_2$, a better performance is achieved when $m_1 < m_2$. One interesting thing to note is that if either m_1 or m_2 values is below one, that is, if the fading conditions on any of the channel link fall below Rayleigh fading, the performance degrades as compared with when either m_1 or m_2 values is one or more than one, that is, when the fading conditions on any of the channel link is Rayleigh or less severe than Rayleigh fading.

Figure 8 shows the BER variations for a BPSK modulated 3×1 and 4×1 systems for different fading conditions, and it was analyzed that the BER improves when $m_1 < m_2$.

No deviations from the results were seen even when $m_1 = m_2$, as in 3×1 and 4×1 system. This can be because of larger number for transmit antennas as compared with a single receive antenna. The MRC combining with larger number of transmit antennas compensated for the higher fading effects when $m_1 < m_2$ thus giving better performance compared with $m_1 = m_2$ as in 2×1 , which gives the best performance when $m_1 = m_2$.

5.5. Results for two-hop decode-amplify-forward relay system for multiple input multiple output system models

Figure 9 shows the BERs for the proposed MIMO system and compares its performance with the conventional MIMO system model for both BPSK and QPSK modulation. The simulations were carried out for 2×2 , 2×3 , 3×2 ,

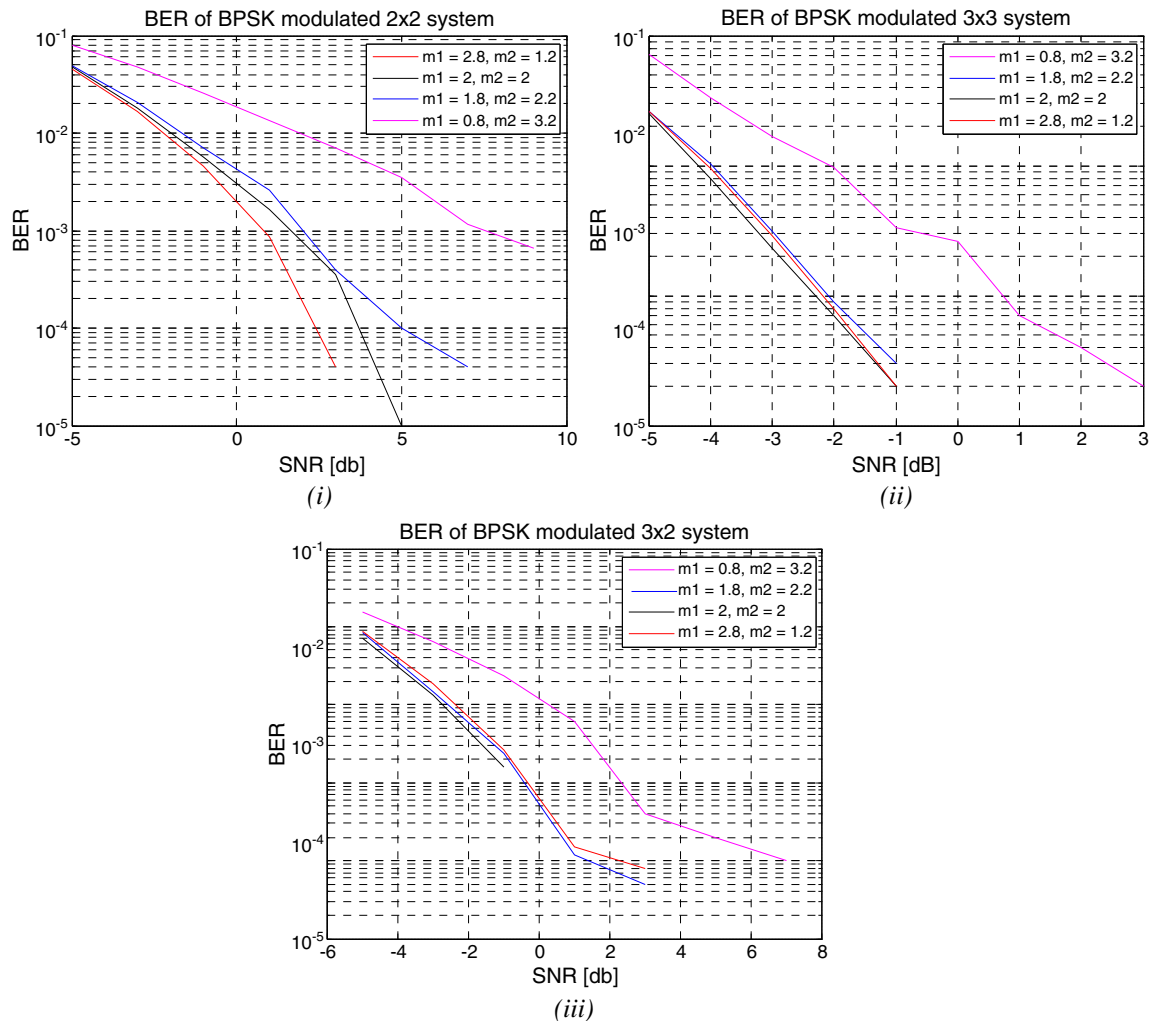


Figure 10. Effect of fading parameter on the performance of the proposed MIMO System. BER of BPSK modulated (i) 2×2 , (ii) 3×3 , and (iii) 3×2 systems.

and 3×3 transmission systems, and it was seen that the added diversity improved the performance of the proposed system by approximately 1 dB. Two spatial data streams are possible when exploiting the 2×2 , 2×3 , and 3×2 system models. However, 3×3 system model is capable of exploiting maximum of three spatial data streams.

Figure 10(i, ii) plots the variations in terms of BER with varying fading conditions on the (T – TR) and (TR – R) links for a 2×2 and 3×3 system model, that is, $N_t = N_r$, respectively. It was analyzed that when $N_t = N_r$ and also N_t and N_r is not very high, for example, 2×2 system model, the BER improves as m_1 is increased, that is, with $m_1 > m_2$, the performance is better, and it improves with increasing value of m_1 . For higher N_t and N_r , for example, 3×3 system model, best performance is achieved when $m_1 = m_2$ and when $m_1 \neq m_2$, better performance is still achieved when $m_1 > m_2$. Thus, a 3×3 model combined the effects of a MISO system model with higher number of transmit antennas and that of a MIMO system model with multiple transmit and receive antennas. Figure 10(iii) plots the BER when $N_t \neq N_r$, and we analyzed that the best performance is achieved when $m_1 = m_2$, and in case $m_1 \neq m_2$, $m_1 < m_2$ gives better performance. For example, with N_t greater than N_r by one, 3×2 and 2×1 system model gives similar performance variations.

6. SUMMARY AND CONCLUSION

In this paper, the BER analysis of SISO, SIMO, MISO, and MIMO wireless system models has been presented, and the importance of exploiting diversity has been put forth. It has been concluded that by increasing the number of diverse paths, the performance of the overall system can be improved. For doing so, an additional TR node placed in between the transmitter and the receiver has been used such that the system behaves as a two-hop DAF relay system. The channel paths between (T – TR), (TR – R), and (T – R) are independent of each other, but they do not vary significantly in terms of their amplitudes and phases. The DAF relay system under study is dynamic as if the TR node fails to work because of any reason or if the system designing is cost effective, the TR node can be bypassed, and the proposed system model can be used like a conventional wireless system model. Also, by placing the TR node at varying distances from the transmitter and the receiver, the following conclusions were derived for various system models:

- For SISO systems, the proposed model gave the best performance when both (T – TR) and (TR – R) links experienced similar fading conditions, that is, when $m_1 = m_2$. However, because of topological limitations when $m_1 = m_2$ may not be possible, better performance is achieved when $m_1 > m_2$.
- For SIMO system models, the proposed SIMO system model performed better than the conventional SIMO model by approximately 2 dB. Also, the proposed SIMO model gave the best performance as long

as $m_1 > m_2$, and the performance sequence was not affected even when $m_1 = m_2$. This has been tested by using 2 and 3 receive antennas, and both models give similar results.

- For MISO system models, the proposed system model gave a better performance than the conventional MISO systems by approximately 1.5 dB. With varying fading conditions on the (T – TR) and (TR – R) links, the system gives the best performance when $m_1 = m_2$ as long as the number of transmit antennas is low, for example, $N_t = 2$ (Figure 7). When the number of transmit antennas become larger, for example, $N_t > 2$, the performance improves with decreasing value of “ m_1 ”, (Figure 8).
- For MIMO system models, the proposed MIMO model with TR node showed the performance improvement of approximately 1 dB. When $N_t = N_r$, a better performance is achieved when $m_1 > m_2$ as long as N_t and N_r is low, and as m_1 is decreased over m_2 , the performance starts to fall, for example, 2×2 . When N_t and N_r is large but still equal, for example 3×3 system, the variations in performance changes, and the best performance is achieved when $m_1 = m_2$ and following the trend of 2×2 model when $m_1 \neq m_2$ giving better results when $m_1 > m_2$. When $N_t > N_r$, the best performance is achieved when $m_1 = m_2$, and the performance starts to decrease with increasing m_1 , for example, 2×1 and 3×2 system models give similar results as $N_t > N_r$.

Thus, we conclude from the simulations performed that the proposed model definitely performs better than the conventional system models. However, the proposed system shows sensitivity towards the number of transmit and receive antennas used and also the fading conditions of (or the distance between) the (T – TR) and (TR – R) channels links. Careful selection of the number of transmit and receive antennas depending on the fading conditions will definitely result in improved performance. Also, the performance of the system is affected by the distance of the TR node from the transmitter and the receiver. Diversity is achieved by exploiting spatial data streams at the transmitter and the receiver, and also by the use of additional TR node. It is expected that the proposed system can be used for state-of-the-art MIMO technologies such as 802.11n and WLAN applications and help reduce multipath distortions because of the use of multiple data ‘spatial streams’.

REFERENCES

1. Hourani H. An overview of diversity techniques in wireless communication systems. *Postgraduate Course in Radio Communications*, 2004–2005.
2. Kalet I. Modern digital modulation techniques for wireless satellite and wireline communications. *Telecommunications Semiconductor Technology Nano*

- Technology*, Annual International Courses, 2012. (copyright © 2012 CEI-Europe AB).
3. Wong K-K, Murdoch RD, Letaief KB. Performance enhancement of multiuser MIMO wireless communication systems. *IEEE Transactions on Communications* 2002; **50**(12): 1960–1970.
 4. Abouda AA, Häggman SG. Effect of mutual coupling on capacity of MIMO wireless channels in high snr scenario. *Progress in Electromagnetics Research* 2006; **65**: 27–40.
 5. Kumar A, Chaudhary A. Channel capacity enhancement of wireless communication using MIMO technology. *International Journal of Scientific & Technology Research* 2012; **1**(2): 91–100.
 6. Bolcskei H, Eth Z. MIMO-OFDM wireless systems: basics, perspectives, and challenges. *IEEE Wireless Communications* 2006; **13**: 31–37.
 7. Schad A, Pesavento M. Multiuser bi-directional communications in cooperative relay networks., In *2011 4th IEEE International Workshop on Computational Advances in Multi-Sensor Adaptive Processing (CAMSAP)*, 13-16 Dec. 2011, San Juan, Puerto Rico, 2011; 217–220.
 8. Goldsmith A, Wicker SB. Design challenges for energy-constrained ad hoc wireless networks. *IEEE Wireless Communications Magazine* 2002; **9**(4): 8–27.
 9. Kaur G, Bhattacharya PP. A survey on cooperative diversity and its applications in various wireless networks. *International Journal of Computer Science and Engineering Survey* 2011; **2**(4): 133–152.
 10. Laneman JN, Tse DNC, Wornell GW. Cooperative diversity in wireless networks: efficient protocols and outage behavior. *IEEE Transactions on Information Theory* 2004; **50**(12): 3062–3080.
 11. Hasna MO, Alouini MS. End-to-end performance of transmission systems with relays over Rayleigh fading channels. *IEEE Transactions on Wireless Communications* 2003; **2**(6): 1126–1131.
 12. Ikki S, Ahmed MH. Performance of decode-and-forward cooperative diversity networks over Nakagami-m fading channels, In *Proceedings of IEEE GLOBECOM'07*, Washington, DC, Nov. 2007; 4328–4333.
 13. Bao X, Li J. Efficient message relaying for wireless user cooperation: decode-amplify-forward (DAF) and hybrid DAF and coded-cooperation. *IEEE Transactions on Wireless Communications* 2007; **6**(11): 3975–3984.
 14. Duong TQ, Zepernick HJ. On the performance gain of hybrid decode-amplify-forward cooperative communications. *EURASIP Journal on Wireless Communications and Networking* 2009; **2009**: Article ID 479463, 10 pages.
 15. Van Der Meulen EC. Three terminal communication channels. *Advances in Applied Probability* Spring 1971; **3**(1): 120–154.
 16. Sato H. Information transmission through a channel with relay. *Technical Report B76-7*, The Aloha System, University of Hawaii, Honolulu, March 1976.
 17. Cover TM, El Gamal AA. Capacity theorems for the relay channel. *Ieee Transactions on Information Theory* 1979; **25**(5): 572–584.
 18. Boyer J, Falconer DD, Yanikomeroglu H. Multi-hop diversity in wireless relaying channels. *IEEE Transactions on Communications* 2004; **52**(10): 1820–1830.
 19. Beaulieu NC, Cheng C. An efficient procedure for Nakagami-m fading simulation, In *Proceedings of IEEE GLOBECOM*, Vol. 6, San Antonio, TX, Nov. 2001; 3336–3342.
 20. Hasna MO, Alouini MS. Performance analysis of two-hop relayed transmissions over Rayleigh fading, In *Proceedings of the Vehicular Technology Conference, VTC 2002-Fall*. 2002 *IEEE 56th*, Vol. 4, 2002; 1992–1996.
 21. Olfat E, Olfat A. Performance of hybrid decode-amplify-forward protocol for multiple parallel relay networks over independent and non-identical flat fading channels. *IET Communications* 2011; **5**(14): 2018–2027.
 22. Can B, Yomo H, De Carvalho E. Hybrid forwarding scheme for cooperative relaying in OFDM based networks, In *Proceedings of IEEE International Conference on Communication*, Vol. 10, Istanbul, Turkey, June 2006; 4520–4525.
 23. Duong TQ, Zepernick H-J. Hybrid decode-amplify-forward cooperative communications with multiple relays, In *Proceedings of IEEE Conference on Wireless Communication and Networking Conference (WCNC)*, 2009; 273–278.
 24. Li Y, Vucetic B. On the performance of a simple adaptive relaying protocol for wireless relay networks, In *Vehicular Technology Conference, 2008. VTC Spring 2008. IEEE*, May 11-14, Singapore, 2008; 2400–2405.
 25. Chen H, Liu J, Zheng L. Performance analysis of SNR-based hybrid decode-amplify-forward cooperative diversity networks over Rayleigh fading channels, In *Wireless Communications and Networking Conference (WCNC)*, *IEEE*, April 18-21, Sydney, NSW, Australia, 2010; 1–6.
 26. Ikki S, Ahmed MH. Performance analysis of cooperative diversity wireless networks over Nakagami-m fading channel. *IEEE Commun. Letters* 2007; **11**(4).
 27. Ko Y-C, Alouini M-S. Estimation of Nakagami-m fading channel parameters with application to optimized transmitter diversity systems. *IEEE Transactions on Wireless Communications* 2003; **2**(2): 250–259.

28. Alamouti SM. A simple transmit diversity technique for wireless communications. *IEEE Journal on Selected Areas in Communications* 1998; **16**(8): 1451–1458.
29. Senaratne D, Tellambura C. Unified performance analysis of two hop amplify and forward relaying, In *Proceedings of IEEE Communications Society, ICC*, 2009.
30. Yang L-L, Chen H-H. Error probability of digital communications using relay diversity over Nakagami-m fading channels. *IEEE Transactions on Wireless Communications* 2008; **7**(5): 1806–1811.
31. Azam MI, Sheikh AUH. Error performance over frequency-selective variable Nakagami fading channel with RAKE reception, In *IEEE 13th International Multi-topic Conference, INMIC*, 14-15 Dec., Islamabad, 2009; 1–6.

wireless communication, multiple input multiple output systems, wireless sensor networks, coding theory, relays, signal processing, channel estimation algorithms and antenna selection.



Jemal H. Abawajy is a professor at the School of Information Technology, Deakin University, Australia. He is a senior member of IEEE and leads the Parallel and Distributed Computing Lab at Deakin University. He is actively involved in funded research and has published more than 200 articles in refereed journals, conferences and book chapters. He is currently the principal supervisor of 10 PhD and co-supervisor of three PhD students. He is on the editorial member of several journals and has guest-edited several journals. He has been a member of the organizing committee for over 100 international conferences serving in various capacity including chair, general co-chair, vice-chair, bestpaper award chair, publication chair, session chair and program committee.

AUTHORS' BIOGRAPHIES



Shivali G. Bansal received her PhD from Deakin University, Australia, in 2012. She is currently working with the RFID research group, Department of Electrical, Computer and Systems Engineering, Monash University, as a research fellow. She is also a visiting scholar at the School of Information

Technology at Deakin University. Her interests are in